

GaAs SAMP Device for Ku-Band Switching

PAUL L. FLEMING, SENIOR MEMBER, IEEE, T. SMITH, MEMBER, IEEE, H. E. CARLSON, MEMBER, IEEE
AND, WILLIAM A. COX, MEMBER, IEEE

Abstract—Switchable attenuating medium propagation (SAMP) devices are coplanar transmission lines on an epitaxial semiconductor (GaAs) substrate. These transmission lines can be switched rapidly between states of high and low attenuation by controlling the width of a depletion layer under the center conductor. SAMP devices can easily be characterized by the use of transmission line theory. They are well suited for use in monolithic microwave integrated circuits (MMIC's). Experimental performance data and theoretical background will be presented.

I. INTRODUCTION

THIS PAPER describes the development of switchable attenuation medium propagation (SAMP),¹ a new type of microwave device. Switching functions in the microwave integrated circuits (MIC's) are generally performed using p-i-n diodes or transistors. The SAMP device is an alternative to the p-i-n diode since neither provides gain. The useful property of the p-i-n diode is that its conductivity can be varied from nearly zero to very high values. The designer treats such a device as a lumped element circuit taking into account the associated parasitic capacitance and inductance. This often results in a narrow-band switch. In contrast, SAMP is a transmission line, and is therefore inherently broad band. Switching in SAMP is accomplished by electronically changing the line between high- and low-loss states. The behavior of a SAMP depends on its transmission line parameters and electrical length, which are selected by the device designer. Given the parameters, well-known transmission line theory may be used to predict performance. Similar to p-i-n diodes and transistors, SAMP devices are very fast. For example, switching times of less than or equal to 1 ns have been achieved.

SAMP has evolved from work on the active medium propagation (AMP) transmission line concept [1]–[3]. However, the operation of SAMP depends on different physics than that of AMP. The AMP device could also be used as a switch; however, for this application, its bilateral gain in the on-state presents impedance matching and stability problems. SAMP is stable, and matching for low VSWR can easily be achieved. SAMP devices also require much less power than AMP's to maintain the on-state.

II. DESIGN AND OPERATING PRINCIPLES

Fig. 1 shows the SAMP device configuration. The GaAs conducting layer is about 5 μm thick and has a carrier concentration of about 10^{15} cm^{-3} . Carrier concentration

Manuscript received August 25, 1979; revised September 11, 1979. This paper is based upon work performed in COMSAT Laboratories under the sponsorship of the Communications Satellite Corporation.

The authors are with COMSAT Laboratories, Clarksburg, MD 20734.

¹Patent pending.

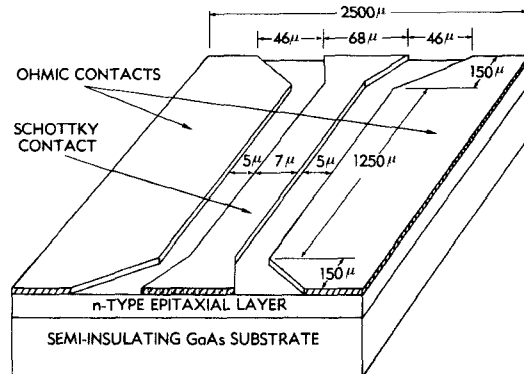


Fig. 1. Geometry of SAMP chip on GaAs material (not to scale).

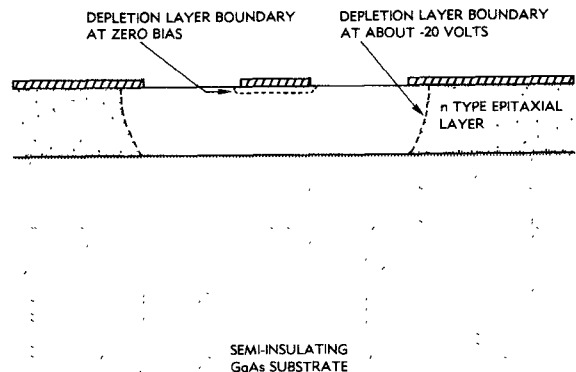


Fig. 2. Cross section of a SAMP showing the positions of the depletion layer edge in the on-state and at zero bias.

is the main factor that determines the off-state loss of the device. In the cross section shown in Fig. 2, the ground planes make ohmic contact to the GaAs epitaxial material. The center conductor is a Schottky barrier. In the on-state, a negative bias is applied to the center conductor causing electrons to be depleted from the GaAs under the gaps, resulting in low-loss transmission. In the off-state, a small positive bias is applied to the center conductor, resulting in high attenuation due to the shunt conductivity across the gaps. The depletion layer width at breakdown depends on the carrier concentration; therefore, an upper limit for carrier concentration is set by the gap width of the coplanar line. GaAs is used because its high electron mobility allows high shunt conductivity per unit length for a given carrier concentration and thus high off-state loss. If silicon were used instead of GaAs about one-half the loss in decibels per millimeter could be achieved as limited by the depletion layer width at breakdown for a given gap width.

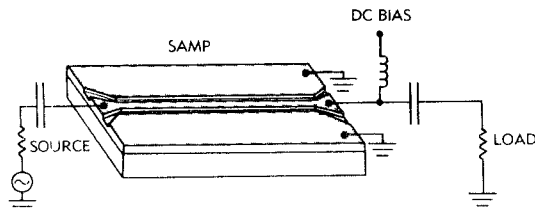


Fig. 3. Circuit diagram of connections to the SAMP chip.

At the input and output ends of the device both the center conductor and the gap width increase. The wide ends of the center conductor serve as bonding pads. The ratio of gap width to center conductor width is kept the same throughout and is chosen for 50Ω characteristic impedance in the lossless limit. Since these end regions are not fully depleted they cause additional on-state loss and reflection.

The typical on-state bias for SAMP devices is -20 to -30 V, center conductor to ground planes, and the on-state current is less than $1\ \mu\text{A}$. For maximum off-state loss, a center conductor bias of about $+0.8$ V is applied. The off-state current is then about $1\ \text{mA}$. If less off-state loss is acceptable, zero bias can be used.

EXPERIMENTAL RESULTS

Measurements were performed with the SAMP devices mounted in a rectangular opening in an alumina MIC board. Fig. 3 is a circuit diagram of the connections to the device. The SAMP conductors are connected to the corresponding coplanar conductors on the MIC board by wire bonding. The MIC board coplanar lines are connected to standard 50Ω SMA microstrip to coaxial connectors. The ground planes of the MIC board have been electroplated with about $100\ \mu\text{m}$ of copper which overhangs the opening for the SAMP as shown in Fig. 4. The copper, which provides a heat sink for the power absorbed by the device, is plated with a thin layer of gold. All the measurement data quoted refer to the circuit between the SMA ports. No correction has been made for any losses between the ports and the SAMP device.

Insertion loss was measured in the 13- to 18-GHz range. Early SAMP devices demonstrate losses from 7 to 10 dB for the on-state and 22 to 25 dB for the off-state. The fairly high on-state loss is mainly due to the series resistance of the center conductor. To reduce the series resistance, $3\ \mu\text{m}$ of gold is electroplated onto the center conductor and ground planes. These devices, designated SAMP-P, exhibit on-state insertion losses ranging from 1.5 to 3 dB and off-state losses from 17 to 20 dB, as shown in Fig. 5.

The VSWR measured in the input coaxial line to a SAMP-P device is 1.4 for the on-state and 2.6 for the off-state. When it is assumed that the tapered end sections are completely undepleted, the theory presented below gives higher VSWR values. However, these sections are partially depleted in the on-state, which should tend to reduce the on-state VSWR. Both off-state and on-state VSWR may be reduced by losses on the MIC board which are not considered in the theory. It was found that tuning discs on the MIC board could equalize the on-state

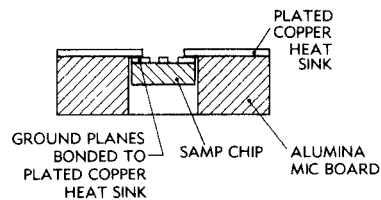


Fig. 4. Cross section of MIC board showing the plated heat sink and the SAMP chip.

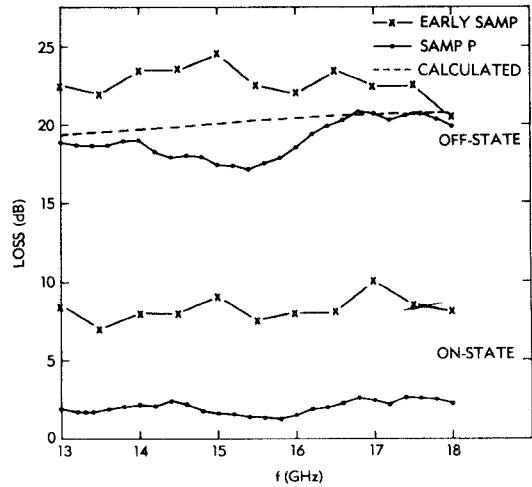


Fig. 5. Insertion loss versus frequency for a mounted early SAMP and for SAMP-P in both on- and off-states, and the computed off-state loss.

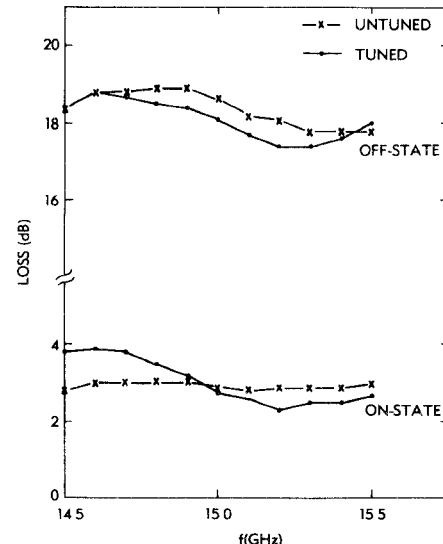


Fig. 6. The effect on insertion loss of tuning to equalize on-state and off-state VSWR at 15 GHz.

and off-state VSWR values to 1.65 at 15 GHz. Fig. 6 shows the effect of this tuning on insertion loss versus frequency.

SAMP-P devices, mounted as described, have switched up to 2-W input power. The switching time is less than or equal to 1 ns, which is the rise and fall time of the pulse generator used to switch the center conductor bias. The on-state carrier to third-order intermodulation products ratio for two carriers in the 11-GHz satellite communications band, separated by 600 kHz, 1 W per carrier, has been measured at 45 dB.

THEORETICAL CONSIDERATIONS

Various design tradeoffs exist for SAMP devices. For example, increasing the shunt conductivity increases both the loss per unit length and the off-state VSWR while decreasing the power handling capability. Increasing the line length increases both the on-off ratio and the on-state loss. Increasing the center conductor width decreases both the on-state loss and characteristic impedance. Suitable choices must be made to meet the requirements of each application.

The parameters of coplanar transmission lines may be calculated using two Schwarz-Christophel conformal transformations. The points of the cross section of Fig. 2 are plotted on the complex Z plane as shown in Fig. 7. Then the transformation given by Wen [4] is applied:

$$W_1 = u_1 + iv_1 = F\left(\frac{Z}{a}, k_1\right) \quad (1)$$

where F is the incomplete elliptic integral of the first kind, modulus k_1 , and

$$k_1 = a/b \quad (2)$$

where a and b are defined in Fig. 9. The inverse transformation is

$$Z = x + iy = a \operatorname{Sn}(W_1, k_1) \quad (3)$$

where Sn is the Jacobian elliptic sine function. Equation (1) results in the map shown in Fig. 8, where K_1 is the complete elliptic integral of the first kind, modulus k_1 , and K'_1 is its complementary complete elliptic integral. This map has the geometry of a parallel-plate strip line cross section, one-half filled with GaAs and the other with air. Since the conductor separation is K'_1 and the width $4K_1$, the inductance per unit length is

$$L = \frac{\mu_0 K'_1}{4K_1} \quad (4)$$

and the capacitance per unit length is

$$C = 2(\epsilon_r + 1)\epsilon_0 \left(\frac{K_1}{K'_1} \right). \quad (5)$$

If it is assumed that center conductor current density is uniform in the Z plane and that the current density versus u_1 in the W_1 plane is the same for both conductors, the following approximate formula for series resistance R per unit length can be obtained

$$R = \left(1 + \frac{k_1}{3} \right) R_0 \quad (6)$$

where R_0 is the resistance per unit length of the center conductor, and k_1 is given by (2).

To find G , the conductance per unit length, the Schwarz-Christophel transformation

$$W_2 = u_2 + iv_2 = F\left[\frac{\sinh(\pi Z/2t)}{\sinh(\pi a/2t)}, k_2\right] \quad (7)$$

where F is defined as for (1), and

$$k_2 = \frac{\sinh(\pi a/2t)}{\sinh(\pi b/2t)} \quad (8)$$

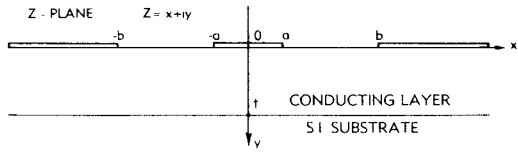


Fig. 7. Cross section of a SAMP device plotted on the complex plane $Z = x + iy$.

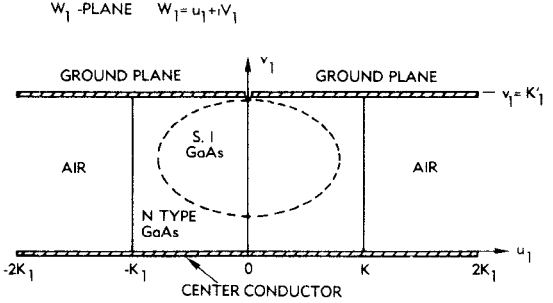


Fig. 8. Conformal map of the coplanar transmission line cross section resulting from the Schwarz-Christophel transformation of (1).

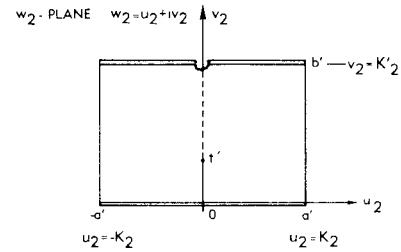


Fig. 9. Conformal map of conducting layer only resulting from the Schwarz-Christophel transformation of (7).

where a , b , and t are defined in Fig. 7 can be used. This maps the active layer into a rectangle as shown in Fig. 9, where K_2 is the complete elliptic integral of the first kind, modulus k_2 , and K'_2 is its complementary complete elliptic integral. With this transformation the substrate disappears into the cut in the W_2 plane shown as a dashed line. The inverse transformation is

$$Z = \left(\frac{2t}{\pi} \right) \operatorname{arcsinh} \left[\sinh \left(\frac{\pi a}{2t} \right) \operatorname{Sn}(W_2, k_2) \right]. \quad (9)$$

The map of Fig. 9 allows calculation of the dc shunt conductance per unit length G_0 in the low-contact resistance limit,

$$G_0 = \frac{2K_2}{\rho K'_2} \quad (10)$$

where ρ is the resistivity of the conducting layer. It is assumed that it is valid to equate this to G , the ac conductance per unit length, without changing L or C . Experimentally, this seems to be a good assumption if the predicted loss due to the shunt conductance is less than about 20 dB/mm. Transmission loss, scattering parameters, and VSWR can be calculated for any frequency from the parameters R , L , G , and C , the length, and source and load impedances by using well-known transmission line formulas. For example,

$$\gamma = \alpha + j\beta = \sqrt{(R + j\omega L)(G + j\omega C)} \quad (11)$$

TABLE I
EXAMPLE OF SAMP CHARACTERISTICS AS A FUNCTION OF G AT 15 GHz

C (mho/cm)	Attenuation (dB/mm)	VSWR	Change Between On- and Off-States		
			Attenuation (dB/mm)	Phase (deg/mm)	Phase (deg/dB)
0	0.77	1.00			
0.01	0.99	1.28	0.22	-0.13	-0.60
0.05	1.87	1.75	1.10	-0.22	-0.20
0.1	2.92	2.22	2.15	0.52	0.24
0.2	4.77	3.01	4.00	3.75	0.94
0.5	8.76	4.79	7.97	16.24	2.04
1.0	13.13	6.86	12.36	34.65	2.80
2.0	19.17	9.78	18.40	63.23	3.44
5.0	30.90	15.56	30.14	122.58	4.07

is the propagation constant. The imaginary part β times the line length gives the phase shift between the ends of the line in radians. The attenuation A in decibels for a line length l with matched source and load is

$$A = 20 \log_{10}(e^{\alpha l}). \quad (12)$$

The characteristic impedance is given by

$$Z_c = R_c + j\omega L_c = \sqrt{\frac{R + j\omega L}{G + j\omega C}}. \quad (13)$$

The above formulas reveal that a line matched for the on-state ($G \approx 0$) is generally mismatched for the off-state ($G \neq 0$), and that there will usually be a phase shift between the on-state and off-state. Table I shows the effect of increasing the off-state G ; the on-state G is taken to be zero. The following parameters are used in this example: $R = 90 \Omega/\text{cm}$, $L = 4.46 \text{ nH/cm}$, and $C = 1.74 \text{ pF/cm}$. The value of R is derived using (6) and assuming approximately one skin depth at 15 GHz in a 7- μm wide center conductor with 5- μm wide gaps using a resistivity of about $5 \mu\Omega\cdot\text{cm}$ (for slightly impure gold). L and C are computed for the same dimensions using 12.95 for the relative dielectric constant of GaAs. The values given are for infinite length, and it is assumed that the source is matched to the on-state ($G = 0$) case. The highest value of G , 5 mho/cm, is probably higher than that which can be achieved in practice if 5- μm gaps must be depleted in the on-state.

The zero phase shift as a function of G depends on the value of R . The frequency dependence of some of the parameters given in Table I for off-state $G = 1 \text{ mho/cm}$ and constant R is shown in Table II.

The propagation constant γ and the characteristic impedance Z_c may be used in constructing a matrix representation of a length of uniform transmission line. The nonuniform end sections of a SAMP may be modeled as a series of short uniform segments. Matrix multiplication gives the matrix representation of the entire cascade. Fig. 5 shows the agreement of the experimental data with computations based on the above theory. Manufacturer's

TABLE II
EXAMPLE OF SAMP CHARACTERISTICS AS A FUNCTION OF F FOR $G = 1 \text{ mho/cm}$

f (GHz)	VSWR	Change Between On- and Off-States		
		Attenuation (dB/mm)	Phase (deg/mm)	Phase (deg/dB)
10	8.45	10.82	30.22	2.79
15	6.86	12.36	34.65	2.80
20	5.92	13.62	36.65	2.70
25	5.27	14.66	37.54	2.56
30	4.79	14.53	37.59	2.42
35	4.23	16.26	37.19	2.29
40	4.13	16.89	36.49	2.16

data on the GaAs wafer and measurements of the SAMP center conductor resistance were used to calculate the SAMP off-state G and R (including skin effect) as a function of frequency. A typical MIC board and connector loss of 1.5 dB was added to obtain the dashed line. This shows good agreement although most of the experimental points show slightly less loss. The 1.5-dB estimate of the MIC board and conductor loss may be high; in some cases this loss is as low as 0.9 dB at 15 GHz. The theory does not consider the effects of distortion of the RF fields due to the shunt currents or the coupling across the SAMP due to nontransmission line modes. The excess variation with frequency of the experimental points is probably attributable to the effects of VSWR on the MIC coplanar line.

CONCLUSION

A new microwave switching device (SAMP), which is a uniform coplanar transmission line, has been described. It is expected that this device, along with the related AMP device, will become a useful MIC component, and will be a useful component for monolithic integrated circuits.

ACKNOWLEDGMENT

The authors are grateful to M. Gardwell of Plessey and A. Cornfeld of COMSAT for growth of the GaAs epitaxial wafers used in this work; J. Reynolds for materials characterization; W. Chang for fabrication of the MIC boards and heat sinks; and Dr. E. S. Rittner for his continued support of this program.

REFERENCES

- [1] P. L. Fleming, T. Smith, H. E. Carlson, and W. A. Cox, "CW operation of AMP," in *Tech. Dig. Int. Electron Devices Meet.* Dec. 5-7, 1977, pp. 93-96, also *IEEE Trans. Electron Devices*, vol. ED-26, pp. 1267-1272, Sept. 1979.
- [2] P. L. Fleming, "The Active Medium Propagation Device," *Proc. IEEE (Letters)*, vol. 63, pp. 1253-1254, Aug. 1975.
- [3] —, "Planar transmission line comprising a material having negative differential conductivity," U.S. Patent 3 975 690.
- [4] C. P. Wen, "Co-planar waveguide: A surface strip transmission line suitable for nonreciprocal gyromagnetic applications," *IEEE Trans. Microwave Theory Tech.*, vol. MTT-17, pp. 1087-1091, Dec. 1969.